Heat Mass Transfer (2013) 49:1357–1366
DOI 10.1007/s00231-013-1179-y

ORIGINAL

Flow and heat transfer of nanofluids over stretching sheet taking into account partial slip and thermal convective boundary conditions

A. Noghrehabadi · R. Pourrajab · M. Ghalambaz

Received: 3 February 2012 / Accepted: 21 May 2013 / Published online: 1 June 2013

Abstract The effect of flow slip on the nanofluid boundary layer over a stretching surface is studied. The present results provide a basic understanding on the effects of the slip boundary condition on heat and mass transfer of nanofluids past stretching sheets subject to a convective boundary condition from below. The results show that an increase of thermophoresis parameter or slip factor would decrease the reduced Nusselt number in some cases.

List of symbols

$(\rho c)_f$	Heat capacity of the fluid
$(\rho c)_p$	Effective heat capacity of the nanoparticle material
Bi	Biot number
c	Constant
D_B	Brownian diffusion coefficient
D_T	Thermophoretic diffusion coefficient
h_f	Heat transfer coefficient of convective heat transfer
k	Thermal conductivity
Le	Lewis number
N	Slip constant
Nb	Brownian motion parameter
Nt	Thermophoresis parameter
Nu	Nusselt number
p	Pressure
Pr	Prandtl number
q_m	Wall mass flux
q_w	Wall heat flux
Re_x	Local Reynolds number
Sh_x	Local Sherwood number
T	Fluid temperature
T_∞	Ambient temperature
T_f	Temperature of the hot fluid
T_w	Temperature at the stretching sheet
u,v	Velocity components along x and y axes
u_w	Velocity of the stretching sheet
x,y	Cartesian coordinates (x axis is aligned along the stretching surface and y axis is normal to it)

Greek symbols

α	Thermal diffusivity
β	Dimensionless nanoparticle volume fraction
η	Similarity variable
θ	Dimensionless temperature
λ	Dimensionless slip factor
ρ_f	Fluid density
ρ_p	Nanoparticle mass density
τ	Parameter defined by ratio between the effective heat capacity of the nanoparticle material and heat capacity of the fluid
ϕ	Nanoparticle volume fraction
ϕ_∞	Ambient nanoparticle volume fraction
ϕ_w	Nanoparticle volume fraction at the stretching sheet
ψ	Stream function

A. Noghrehabadi (✉) · R. Pourrajab · M. Ghalambaz
Department of Mechanical Engineering, Shahid Chamran University of Ahvaz, Ahvaz, Iran
e-mail: a.r.noghrehabadi@gmail.com; noghrehabadi@scu.ac.ir

R. Pourrajab
e-mail: r-pourrajab@mscstu.scu.ac.ir

M. Ghalambaz
e-mail: m.ghalambaz@gmail.com

1 Introduction

The boundary layer flow over a moving continuous solid surface is an important type of flow, which occurs in several engineering processes. For example, in industry the heat-treated materials travel between a feed roll and a wind-up roll while they are subject to heat transfer with a fluid. Another example is the materials manufactured by extrusion of plastic sheets [1]. These engineering processes can be modeled as a stretching sheet. The stretching sheet phenomena occur in many other applications such as: paper production, glass blowing, metal spinning [2], polymer engineering [3], cooling of metallic sheets and crystal growing [1, 3]. In the mentioned applications, the heat transfer rate in the boundary layer over stretching sheet is important because the quality of the final product depends on the heat transfer rate between the stretching surface and the fluid during the cooling or heating process [4]. Therefore, the choice of a suitable cooling/heating liquid is essential as it has a direct impact on the rate of heat transfer.

In recent years, the heat transfer enhancement of nanofluid has been proposed as a route for surpassing the performance of heat transfer rate in liquids currently available [5]. Nanofluid is described as a fluid in which the solid nanoparticles with the length scales of nanometers are suspended in a conventional heat transfer fluid. It has been demonstrated that the addition of highly conductive particles can significantly enhance the thermal conductivity of the pure base fluid. For example, it was reported that the effective thermal conductivity of an ethylene–glycol-based nanofluid which contains nano size copper particles with diameters less than 10 nm increased by up to 40 at 0.3 % vol. of dispersed particles [6]. An excellent review of nanofluid physics and developments can be found in [7, 8] and the book of Das et al. [9]. The current experimental data shows that the force-convection enhances in the presence of nanoparticles [10], and the enhancement increases with the increase of nanoparticle volume fraction [11].

Currently, there are two main approaches in the modeling of heat transfer convection in nanofluids. In the first approach, the nanofluid can be modeled as the common pure fluid where the conventional equations of mass, momentum and energy can be used. In the mentioned models, it is assumed that the enhancement of convective heat transfer is just because of the enhancement in thermophysical properties, which are affected by nanoparticle volume fraction and nanoparticle properties. In these models, the nanoparticles are in thermal equilibrium with fluid molecules, and there is not any slip velocity between the nanoparticles and fluid molecules. Thus, a uniform mixture of nanoparticles is considered for the nanofluid [5, 11–13].

In the second approach, it is believed that in the convection of nanofluids there are several slip mechanisms, so the volume fraction of nanoparticles in the nanofluid may not be uniform. A comprehensive survey in the field of convective transport in nanofluids has been done by Buongiorno [14]. He demonstrated that the high heat transfer coefficients in the nanofluids cannot be explained adequately by thermal dispersion [15], nanoparticle rotation [16] or increase in turbulence intensity of nanoparticles [17] as proposed in the literatures. Buongiorno considered seven slip mechanisms which can produce a relative velocity between the nanoparticles and the base fluid. Of all of these seven mechanisms, only thermophoresis and Brownian diffusion were found to be important. Later, Buongiorno [14] developed an analytical model for convective transport in nanofluids in which Brownian motion and thermophoresis effect were considered.

Sakiadis [18] studied the boundary layer behavior for the sheet moving with a constant velocity in a viscous fluid. The analytical solution for steady stretching of the surface was given by Crane [19]. After this pioneering work, various aspects of the problem including magneto hydrodynamic flows [20], non-Newtonian fluids [21], nanofluids [22–24], flows with chemical reactions [25], and also different hydrodynamic and thermal boundary conditions have been investigated.

Some of the researchers considered different idealized thermal boundary conditions for the sheet surface. Gupta and Gupta [26] analyzed heat and mass transfer over a stretching sheet with constant surface temperature. Different thermal boundary conditions such as power-law surface temperature and power-law surface heat flux were discussed by Fang [27]. Cortell [28] investigated the viscous flow and heat transfer over a stretching sheet prescribed power law surface temperature. However, when the sheet is prescribed to a convective fluid from below, the consideration of constant or variable temperature/heat flux is not a realistic boundary condition in many engineering applications of stretching sheet. In this case, the convective boundary condition is a more realistic thermal boundary condition. Recently, number of researchers examined the convective boundary condition. Aziz [29] considered the classical problem of hydrodynamic and thermal boundary layers over a flat plate in a uniform stream of fluid. Aziz obtained a similarity solution for laminar thermal boundary layer over a flat plate with a convective surface boundary condition. Later, Magyari [30] introduced an analytical approach for heat equation which has been implemented in the work of Aziz [29]. Hamad et al. [31] investigated the heat and mass transfer of boundary layer stagnation-point flow over a stretching sheet in a porous medium saturated by a nanofluid using a lie group analysis. Ishak [32] obtained a similarity solution of flow and heat transfer over a permeable surface with a convective boundary condition. The forced convection of a uniform stream flow over a flat surface with a convective surface boundary condition has been theoretically analyzed by Merkin and Pop [33]. Yao et al. [34] studied heat transfer in the stretching sheet problem with convective boundary condition, and they obtained an exact solution in the form of an incomplete Gamma function. They reported that the convective boundary condition results in temperature slip at the wall, which it is greatly affected by the Prandtl number and the wall stretching parameters. They found that the temperature profiles are quite different from the prescribed wall temperature cases.

Beyond the temperature boundary conditions, many researchers studied the different aspects of hydrodynamic boundary conditions including permeable stretching sheet and partial slip velocity on the sheet surface. The slip flow problem of laminar boundary layer is of considerable practical interest. Microchannels which are at the forefront of today's turbomachinery technologies, are widely being considered for cooling of electronic devices, micro heat exchanger systems, etc. If the characteristic size of the flow system is small or the flow pressure is very low, slip flow happens [35]. Wang [36] reported that the partial slip between the fluid and the moving surface may occur in situations that the fluid is particulate such as emulsions, suspensions, foams and polymer solutions. Wang [37], Andersson [38] and Ariel [39] employed a partial slip boundary condition to study the flow of a pure fluid over a stretching sheet. The effects of partial slip on the steady flow of an incompressible, electrically conducting third grade fluid past a stretching sheet has been examined by Sahoo and Do [40]. Hayat et al. [41] analyzed the effect of the slip boundary condition on the magneto hydrodynamic flow and heat transfer over a stretching sheet. The influence of partial slip, thermal radiation and temperature dependent fluid properties on the hydro-magnetic fluid flow and heat transfer over a flat plate with heat generation has been analyzed by Das [42].

Bocquet and Barrat [43] examined the effect of flow boundary conditions from nano to micro scales near the solid interfaces. They briefly discussed the mechanisms of surface slip and heat transfer on the interface. Bachok et al. [44] extended the Blasius and Sakiadis problems in nanofluids. Yacob et al. [5] investigated boundary layer flow past a stretching sheet with a convective boundary condition at the surface for two types of nanofluids, namely, Cu–water and Ag–water. They discussed the effect of the convective parameter on the heat transfer characteristics, but they did not consider the effect of Brownian motion and thermophoresis in their study. They found that the heat transfer rate at the surface increases with the increase of the nanoparticle volume fraction while it decreases with the increase of the convective parameter.

Recently, the Buongiorno's model [14] has been used by Kuznetsov and Nield [45] to study the influence of nanoparticles on the natural convection boundary layer flow past a vertical plate. Khan and Pop [22] analyzed the boundary-layer flow of a nanofluid past a stretching sheet in a model in which the Brownian motion and thermophoresis effects have been taken into account. Hassani et al. [46] analytically examined the work of Khan and Pop [22]. Makinde and Aziz [47] examined the effect of a convective boundary condition on the boundary layer flow of nanofluids past a linear stretching sheet in order to obtain the more realistic solution where non-isothermal conditions at the flat sheet are present. They found that the local concentration of nanoparticles increases as the convection Biot number increases. The entropy generation [48] and magnetic effects [49] also are analyzed for nanofluid flow and heat transfer over stretching sheets. Rana and Bhargava [50] considered a nonlinear velocity for the sheet, and they analyzed the flow and heat transfer of a nanofluid over it.

To the best of authors' knowledge, there is not any investigation to address the effect of the slip boundary condition on the heat transfer characteristics of nanofluid flow over stretching sheet prescribed convective boundary conditions in a model in which the dynamic effects of nanoparticles are taken into account. The present study aims to examine the effect of the slip boundary condition on the heat transfer characteristics of stretching sheet which is subjected to convective heat transfer on its surface in the presence of nanoparticles and their dynamic effects.

2 Governing equations

Consider a two-dimensional incompressible and steady state viscous flow of a nanofluid over a continuously stretching surface. The velocity of surface is linear, and is taken as $U_{w(x)} = c.x$ where c is a constant, and x is the coordinate component measured along the stretching surface. A flow with the convective heat transfer coefficient of h_f and temperature of T_f is flowing below the stretching sheet. The scheme of physical configuration is depicted in Fig. 1. It is worth mentioning that there are three distinct boundary layers, namely, hydrodynamic boundary layer (velocity), thermal boundary layer (temperature) and concentration boundary layer (nano particle volume fraction)

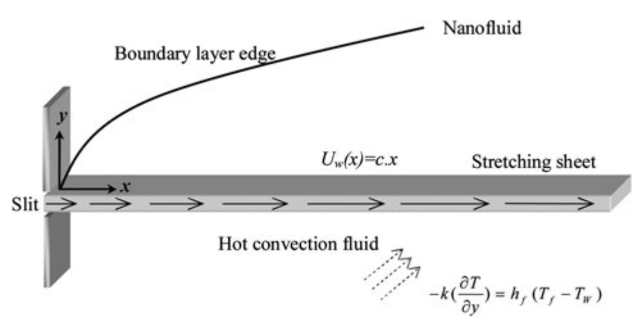

Fig. 1 Scheme of physical configuration of stretching sheet

over the sheet. However, in the Fig. 1 only single boundary layer is plotted to avoid congestion. Here, the nanofluid flows at $y = 0$ where y is the coordinate measured normal to the stretching surface.

In the continuum modeling of fluidic transport no-slip boundary condition is sometimes assumed, which means that the fluid velocity component is assumed to be zero relative to the solid boundary [51]. For nanofluids, however, this assumption no longer holds [51], and a certain degree of tangential slip must be allowed [51, 52]. Considering the Navier's condition, the velocity slip is assumed to be proportional to the local shear stress at the sheet surface [37]. The fraction of nanoparticles ϕ_w is assumed constant at the stretching surface. The stretching sheet surface temperature T_w, which will be evaluated later, is the result of a convective heating process depending to temperature of hot convective fluid below the stretching sheet (T_f) and convective heat transfer coefficient (h_f).

When y attends to infinity, the values of the temperature and nanoparticle fraction attend to the constant values of T_∞ and ϕ_∞ in the quiescent part of the nanofluid, respectively. ϕ and T indicate the fraction of nanoparticles and the temperature of flow, respectively. For nanofluids, by considering the dynamic effects of the nano particles and applying the boundary layer approximations the Boungiorno's [14] convective transport equations in the Cartesian coordinate system of x and y can be written as follows [22, 47]:

$$\frac{\partial u}{\partial x} + \frac{\partial v}{\partial y} = 0 \tag{1}$$

$$u\frac{\partial u}{\partial x} + v\frac{\partial u}{\partial y} = -\frac{1}{\rho_f}\frac{\partial p}{\partial x} + \nu\nabla^2 u \tag{2}$$

$$u\frac{\partial v}{\partial x} + v\frac{\partial v}{\partial y} = -\frac{1}{\rho_f}\frac{\partial p}{\partial y} + \nu\nabla^2 v \tag{3}$$

$$u\frac{\partial T}{\partial x} + v\frac{\partial T}{\partial y} = \alpha\nabla^2 T + \tau\left\{D_B\nabla\phi\cdot\nabla T + \frac{D_T}{T_\infty}\nabla T\cdot\nabla T\right\} \tag{4}$$

$$u\frac{\partial \phi}{\partial x} + v\frac{\partial \phi}{\partial y} = D_B\nabla^2\phi + \left(\frac{D_T}{T_\infty}\right)\nabla^2 T \tag{5}$$

subject to the following boundary conditions at the sheet,

$$v = 0, \quad u = U_W(x) - U_S, \quad -k\left(\frac{\partial T}{\partial y}\right) = h_f(T_f - T), \quad \phi = \phi_W, \quad at\, y = 0 \tag{6}$$

and the following boundary conditions at the far field (i.e. $y \to \infty$),

$$v = u = 0, \quad T = T_\infty, \quad \phi = \phi_\infty, \tag{7}$$

Here, u and v are the velocity components along the axis x and y respectively. p is the fluid pressure, α is the thermal diffusivity, k is the thermal conductivity of fluid, ν is the kinematic viscosity, ρ_f is the density of the base fluid, ρ_p is the density of the particles, U_s is the velocity slip at the wall, D_B is the Brownian diffusion coefficient, and D_T is the thermophoresis diffusion coefficient. $\tau = (\rho c)_p/(\rho c)_f$ is the ratio of the effective heat capacity of the nanoparticle material and heat capacity of the fluid, ρ is the density and ϕ is rescaled nanoparticle volume fraction and ∇^2 is the Laplace operator in Cartesian coordinates.

In order to obtain similarity solution for Eqs. (1)–(5), the stream function and dimensionless variables can be introduced in the following form,

$$\psi = \sqrt{c\nu}\, f(\eta), \quad \eta = y\sqrt{c/\nu} \tag{8a}$$

$$\beta(\eta) = \frac{\phi - \phi_\infty}{\phi_W - \phi_\infty}, \quad \theta(\eta) = \frac{T - T_\infty}{T_f - T_\infty} \tag{8b}$$

The stream function ψ can be defined as $u = \partial\psi/\partial y$, $v = -\partial\psi/\partial x$, so that Eq. (1) is satisfied identically. The pressure outside the boundary layer in quiescent part of flow is constant; and the flow occurs only due to the stretching of the sheet; and hence, the pressure gradient can be neglected. Considering the usual boundary layer approximations, $u >> v$, $\frac{\partial u}{\partial y} >> \frac{\partial u}{\partial x}, \frac{\partial v}{\partial x}, \frac{\partial v}{\partial y}$, the momentum equation in y direction reduces to $\frac{\partial P}{\partial y} = 0$. By applying the introduced similarity transforms, Eq. (8a, b), on the remaining governing Eqs. (2), (4), (5) the following set of ordinary differential equations are obtained,

$$f''' + ff'' - f'^2 = 0, \tag{9}$$

$$\frac{1}{pr}\theta'' + f\theta' + Nb\beta'\theta' + Nt\theta'^2 = 0, \tag{10}$$

$$\beta'' + \frac{Nt}{Nb}\theta'' + Le\, f\,\beta' = 0, \tag{11}$$

Here, by using the boundary layer approximations and introducing the Navier's condition one may obtain,

$$u - U_W(x) = N\rho\nu\frac{\partial u}{\partial y} = U_S \tag{12}$$

where ρ is the density and N is a slip constant. By applying the similarity transforms, the Eq. (12) is reduced to,

$$f'(0) - 1 = \lambda f''(0), \tag{13}$$

where $\lambda = N\rho(c\nu)^{1/2}$ is the dimensionless slip factor. Performing introduced similarity transforms (i.e. Eq. (8)) on the remaining boundary conditions Eqs. (6), (7) the transformed boundary conditions are obtained which can be summarized as below,

$$At\,\eta = 0: \quad f = 0, \quad f' = 1 + \lambda f'', \quad \theta' = Bi(\theta - 1), \quad \beta = 1 \tag{14}$$

$$At\,\eta \to \infty: \quad f' = 0, \quad \theta = 0, \quad \beta = 0 \tag{15}$$

In the above equations, primes denote differentiation with respect to η. The parameters of Pr, Le, Nb, Nt and Bi are defined by,

$$Pr = \frac{v}{\alpha}, Le = \frac{v}{D_B}, Nb = \frac{(\rho c)_P D_B(\phi_W - \phi_\infty)}{(\rho c)_f v},$$
$$Nt = \frac{(\rho c)_P D_T(T_f - T_\infty)}{(\rho c)_f v T_\infty}, Bi = \frac{h_f\sqrt{v/c}}{k} \tag{16}$$

where Pr, Le, Nb, Nt and Bi denote the Prandtl number, Lewis number, Brownian motion parameter, thermophoresis parameter and Biot number, respectively. Consider a case which Nb and Nt are equal to zero and Biot number attends to infinity. The problem reduces to the classical problem of flow and heat transfer due to a stretching surface in a viscous fluid with constant wall temperature [36, 37, 40]. In this case, the boundary value problem for β becomes ill-posed without physical meaning.

The quantities of local Nusselt number (Nu_x) and Sherwood number (Sh_x) as important parameters in heat and mass transfer can be introduced as,

$$Nu_x = \frac{xq_W}{k(T_W - T_\infty)}, \quad Sh_x = \frac{xq_m}{D_B(\phi_W - \phi_\infty)} \tag{17}$$

where q_w is the wall heat flux and q_m is the wall mass flux. Using the similarity transforms introduced in Eq. (8), one may obtain,

$$Re_x^{-1/2}Nu_x = -\theta'(0), \quad Re_x^{-1/2}Sh_x = -\beta'(0) \tag{18}$$

where $Re_x = u_w(x)x/v$ is the local Reynolds number based on the stretching surface velocity, $u_w(x)$. Kuznetsov and Nield referred the value of $Re_x^{-1/2}Nu_x$ as the reduced Nusselt number, and the value of $Re_x^{-1/2}Sh_x$ as reduced Sherwood number [45]. Also, Khan and Pop [22] and Makinde and Aziz [47] used these names in their papers. It is worth mentioning that Wang [36] and Andersson [38] obtained an exact solution for Eq. (9) subject to the boundary conditions Eqs. (14) and (15).

3 Results and discussion

The exact solution of momentum equation, Eq. (9), subject to the boundary conditions of Eqs. (14) and (15) is proposed by Andersson [38] as follow:

$$f(\eta) = \gamma(1 - \exp(-\gamma\eta)) \tag{19}$$

where γ is the real and positive root of $\lambda\gamma^3 + \gamma^2 - 1 = 0$.

Using the exact solution (Eq. (19)), the set of ordinary differential equations (Eqs. (10) and (11)) subject to the boundary conditions (Eqs. (14) and (15)) are solved numerically for various ranges of the slip boundary condition and for different values of the Prandtl number, Lewis number, Brownian motion parameter, thermophoresis parameter and Biot number. Numerical results are obtained using Runge–Kutta–Fehlberg method [53, 54]. The most crucial factor of the solution is to choose the appropriate finite value of η_∞. Thus, to estimate the value of η_∞, it increased from initial value of 15 to the evaluated values of $\theta'(0)$ and $\beta'(0)$ which they differ only after desired significant digit.

The values of Biot number (Bi) are chosen as less than unit, higher than unit ($Bi = 10$) and very high ($Bi = 1{,}000$). The results of increase of the Biot number from very low to very high values show that the value of $Bi = 1{,}000$ can accurately simulate the isothermal boundary condition which has been previously considered by Khan and Pop [22] with no slip boundary condition. Therefore, $Bi = 1{,}000$ is considered as the physical infinity of the problem where the wall temperature is very close to the hot fluid temperature T_f. The values of slip factor (λ) are chosen as zero (no slip), between zero and unit and a value larger than unit ($\lambda = 1.5$). This selected range of the slip parameters is in good agreement with works of Hamad et al. [55], Wang [36, 37]. Since most nanofluids examined to date have large values for the Lewis number $Le > 1$ [56], the values of $Le = 5$ and 10 have been examined in the present study. The choice of the values for Nb and Nt was dictated by the fact that these values were used by Khan and Pop [22] and Makinde and Aziz [47] for the flow of nanofluid over an stretching sheet.

Table 1 shows the variation of the reduced Nusselt number (Nur) for different values of Nb, Nt, Le and λ when $Pr = 1.0$ and $Pr = 10$. Table 2 shows the variation of reduced Sherwood number for the same parameters as Table 1. Results of Table 1 demonstrate that increase of Biot number increases the reduced Nusselt number while the increase of either thermophoresis parameter or slip factor decreases the reduced Nusselt number for the selected range of Prandtl and Lewis numbers. The results of Table 2 show that the increase of the slip factor decreases the reduced Sherwood number, but the variation of other remaining parameters has different effects on reduced Sherwood number.

Profiles of $\theta(\eta)$ and $\beta(\eta)$ for selected values of the slip factor (λ), Nb and Nt are shown in Figs. 2 and 3, respectively, when $Pr = 5$, $Le = 5$ and $Bi = 0.1$. These figures show the effect of the slip boundary condition on the non-dimensional temperature and concentration distribution profiles. These figures also show that increase of the slip factor increases the magnitude of non-dimensional temperature and concentration distribution. The Brownian motion tends to uniform the concentration of nanoparticles, and the thermophoresis force tends to move nanoparticles

Table 1 Variation of reduced Nusselt number—$\theta'(0)$ with *Nb*, *Nt, Le*, *Pr, Bi* and λ

			$Le = 5$				$Le = 10$			
			$\lambda = 0.1$		$\lambda = 1$		$\lambda = 0.1$		$\lambda = 1$	
Pr	*Nb*	*Nt*	$Bi = 0.1$	$Bi = 10$	$Bi = 0.1$	$Bi = 10$	$Bi = 0.1$	$Bi = 10$	$Bi = 0.1$	$Bi = 10$
		0.1	0.08363	0.47065	0.08012	0.37544	0.08353	0.46632	0.08000	0.37195
	0.1	0.3	0.08343	0.43555	0.07984	0.34695	0.08332	0.42938	0.07970	0.34197
		0.5	0.08323	0.40356	0.07955	0.32107	0.08309	0.39597	0.07939	0.31495
		0.1	0.08135	0.40478	0.07748	0.32246	0.08103	0.39591	0.07711	0.31533
1.0	0.3	0.3	0.08110	0.37410	0.07713	0.29765	0.08075	0.36407	0.07673	0.28960
		0.5	0.08084	0.34622	0.07677	0.27517	0.08047	0.33536	0.07633	0.26648
		0.1	0.07878	0.34680	0.07454	0.27595	0.07820	0.33501	0.07389	0.26649
	0.5	0.3	0.07846	0.32014	0.07411	0.25446	0.07785	0.30772	0.07340	0.24452
		0.5	0.07813	0.29599	0.07365	0.23505	0.07748	0.28318	0.07290	0.22481
		0.1	0.09347	1.01455	0.09185	0.81483	0.09259	0.85606	0.09075	0.68511
	0.1	0.3	0.09323	0.63282	0.09146	0.50199	0.09220	0.49193	0.09013	0.38955
		0.5	0.09295	0.40811	0.09102	0.32239	0.09174	0.30726	0.08939	0.24269
		0.1	0.08333	0.37491	0.07961	0.29789	0.07600	0.23713	0.07107	0.18799
10	0.3	0.3	0.08156	0.21804	0.07700	0.17247	0.07176	0.12917	0.06522	0.10211
		0.5	0.07918	0.13723	0.07335	0.10841	0.06538	0.07962	0.05651	0.06291
		0.1	0.05662	0.10802	0.05025	0.08549	0.03716	0.05166	0.03140	0.04084
	0.5	0.3	0.04778	0.06123	0.04037	0.04839	0.02582	0.02782	0.02082	0.02198
		0.5	0.03714	0.03826	0.02987	0.03023	0.01721	0.01712	0.01360	0.01353

Table 2 Variation of reduced Sherwood number—$\beta'(0)$ with *Nb*, *Nt*, *Le*, *Pr*, *Bi* and λ

			$Le = 5$				$Le = 10$			
			$\lambda = 0.1$		$\lambda = 1$		$\lambda = 0.1$		$\lambda = 1$	
Pr	*Nb*	*Nt*	$Bi = 0.1$	$Bi = 10$	$Bi = 0.1$	$Bi = 10$	$Bi = 0.1$	$Bi = 10$	$Bi = 0.1$	$Bi = 10$
		0.1	1.46505	1.31550	1.15203	1.03805	2.18059	2.07238	1.71885	1.63642
	0.1	0.3	1.39993	1.01401	1.08997	0.79834	2.13272	1.86377	1.67333	1.47071
		0.5	1.33620	0.78474	1.02961	0.61677	2.08633	1.71780	1.62960	1.35532
		0.1	1.48901	1.45386	1.17502	1.14844	2.19926	2.17791	1.73674	1.72064
1.0	0.3	0.3	1.47119	1.38271	1.15817	1.09194	2.18808	2.13826	1.72623	1.68919
		0.5	1.45392	1.33099	1.14199	1.05103	2.17750	2.11440	1.71642	1.67039
		0.1	1.49390	1.48014	1.17970	1.16938	2.20312	2.19740	1.74043	1.73617
	0.5	0.3	1.48574	1.45251	1.17206	1.14748	2.19954	2.18862	1.73712	1.72922
		0.5	1.47798	1.43408	1.16489	1.13292	2.19637	2.18669	1.73430	1.72775
		0.1	1.45032	1.06216	1.13685	0.83523	2.17463	2.03292	1.71267	1.60633
	0.1	0.3	1.35870	1.08973	1.04828	0.86676	2.12063	2.37782	1.66219	1.88498
		0.5	1.27306	1.54916	0.96757	1.23229	2.07731	2.86679	1.62573	2.27062
		0.1	1.49987	1.52998	1.18558	1.20920	2.22686	2.30011	1.76316	1.81774
10	0.3	0.3	1.51068	1.67152	1.19810	1.32152	2.28692	2.48926	1.82278	1.96731
		0.5	1.53439	1.81439	1.22649	1.43430	2.37658	2.62694	1.91164	2.07595
		0.1	1.52145	1.55136	1.20484	1.22584	2.25179	2.27692	1.78238	1.79909
	0.5	0.3	1.58157	1.64854	1.25851	1.30267	2.34971	2.38658	1.86262	1.88573
		0.5	1.65543	1.72272	1.31976	1.36124	2.43146	2.45810	1.92593	1.94222

from hot to cold areas. Increase of *Nb* and *Nt* increases the movement of nanoparticles away from the sheet surface and consequently increases the magnitude of temperature profiles and concentration distribution profiles (as seen in Figs. 2, 3). Increase of slip factor increases the magnitude of both thermal and concentration boundary layer thickness.

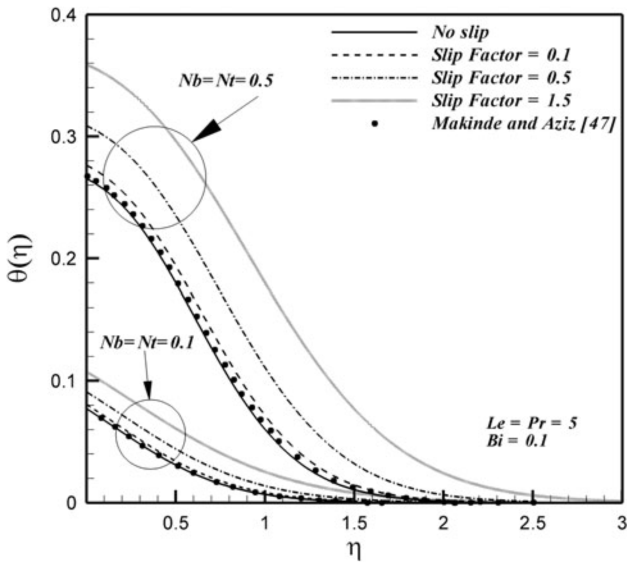

Fig. 2 Effect of slip factor, *Nt* and *Nb* on temperature profiles for $Pr = 5$, $Le = 5$, $Bi = 0.1$

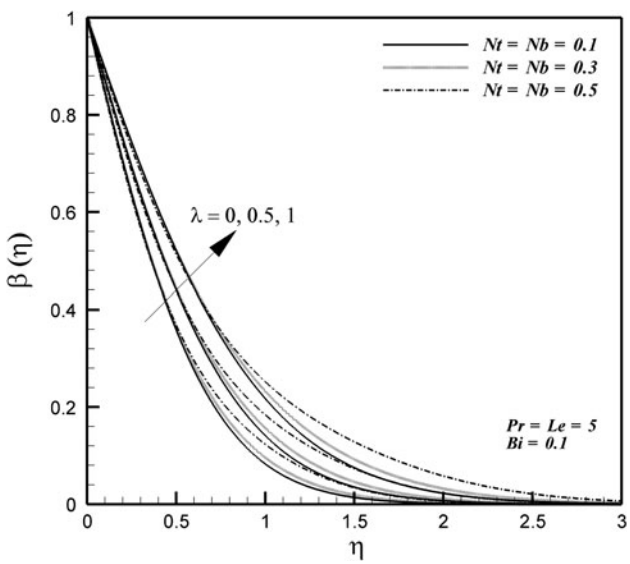

Fig. 3 Effect of slip factor, *Nt* and *Nb* on concentration profiles for $Pr = 5$, $Le = 5$, $Bi = 0.1$

For a typical case with $Pr = 5$, $Le = 5$ and $Bi = 0.1$, the dependent similarity variables $\theta(\eta)$ and $\beta(\eta)$ are plotted for different values of slip factors λ and Biot number parameter Bi in the Figs. 4 and 5, respectively. Figure 4 shows that increase of the slip factor λ or Biot number Bi increases the magnitude of non-dimensional temperature profiles. The stronger convection (higher Biot number) results in higher surface temperatures and consequently the higher values of temperature profiles. Increase of the slip factor decreases the tendency of the nanofluid to remove the heat away from the plate and consequently causes the higher values of temperature profiles. Figure 4 also depicts

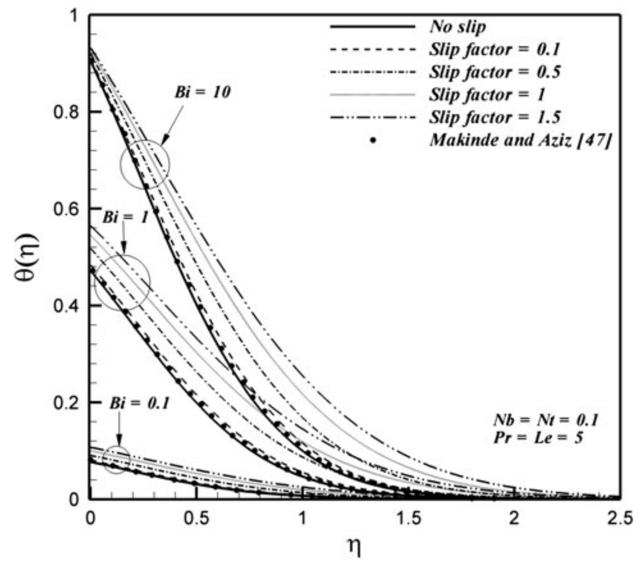

Fig. 4 Effect of slip factor and *Bi* on temperature profiles for $Nb = Nt = 0.1$, $Pr = Le = 5$

that for the small ($Bi = 0.1$) and large ($Bi = 10$) values of Biot number the effect of the slip factor λ on the wall values of non-dimensional temperature profiles $\theta(0)$ is less than it for middle values of Biot number ($Bi = 1$). Increase of the Biot number or slip factor increases the thermal boundary layer thickness and wall temperature values $\theta(0)$. Increase of thermal boundary layer thickness with the increase of the slip factor is due to the fact that the flow of fluid in the boundary layer is in results of the stretching of the sheet. Therefore, increase of the slip factor decreases the flow motion and consequently increases the thickness of thermal and concentration boundary layers. Figure 5 reveals that profiles of $\beta(\eta)$ for all selected values of Biot number and slip factor take value of one on the sheet surface, and they tends to zero as η tends to infinity. This figure depicts that increase of Biot number or increase of the slip factor increases the values of $\beta(\eta)$. It is worth noticing that in the case of ($\lambda \to 0$) the present study reduces to the work of Makinde and Aziz [47]. In the Figs. 2 and 4, the non-dimensioanl temperature profiles (in the case of $\lambda \to 0$) are compared with the results reported by Makinde and Aziz [47]. Similarly, in the Fig. 5, the non-dimensioanl concentration profiles (in the cases of $\lambda \to 0$) are compared with the results reported by Makinde and Aziz [47]. These figures show that the results of present study are in good agreement with the previous study.

The variation of dimensionless heat transfer rate (i.e. reduced Nusselt number) and dimensionless mass transfer rate (i.e. reduced Sherwood number) respect to thermophoresis parameter for different values of Biot number and slip factor when $Pr = 10$, $Le = 10$ and $Nb = 0.1$ are shown in Figs. 6 and 7. According to Fig. 6 the

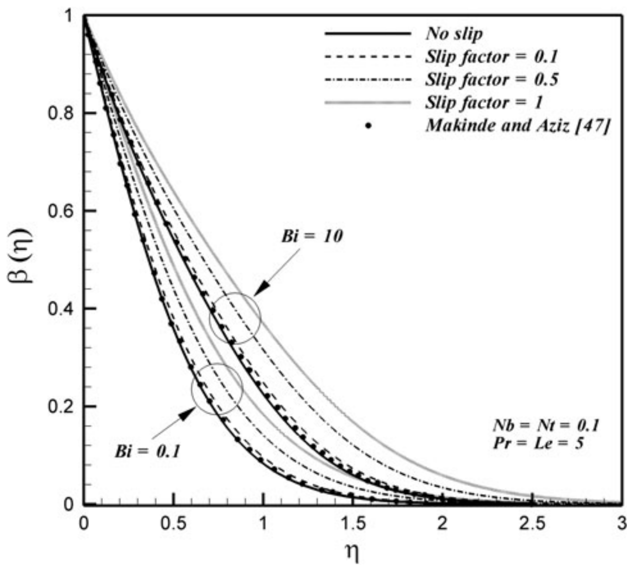

Fig. 5 Effect of slip factor and Bi on concentration profiles for $Nb = Nt = 0.1$, $Pr = 5$, $Le = 5$

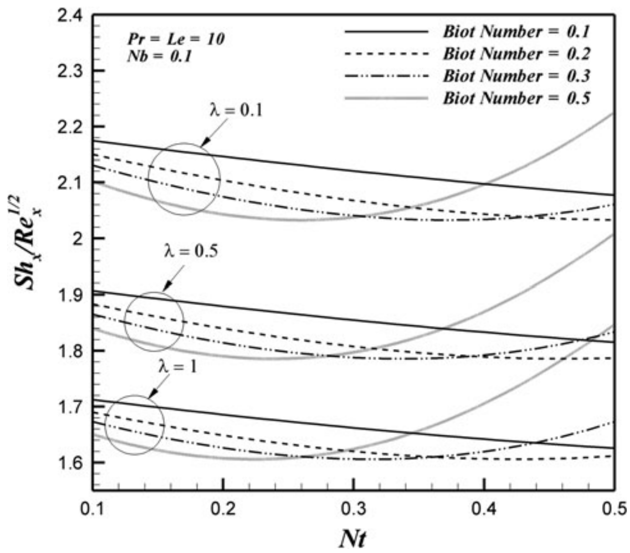

Fig. 7 Effects of slip factor, biot number and thermophoresis parameter on the dimensionless concentration rates for $Pr = 10$, $Le = 10$ and $Nb = 0.1$

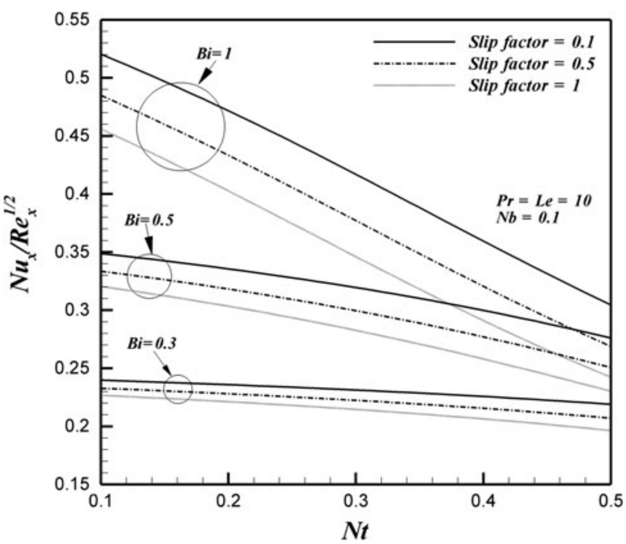

Fig. 6 Effects of slip factor, biot number and thermophoresis parameter on the dimensionless heat transfer rates for $Pr = 10$, $Le = 10$ and $Nb = 0.1$

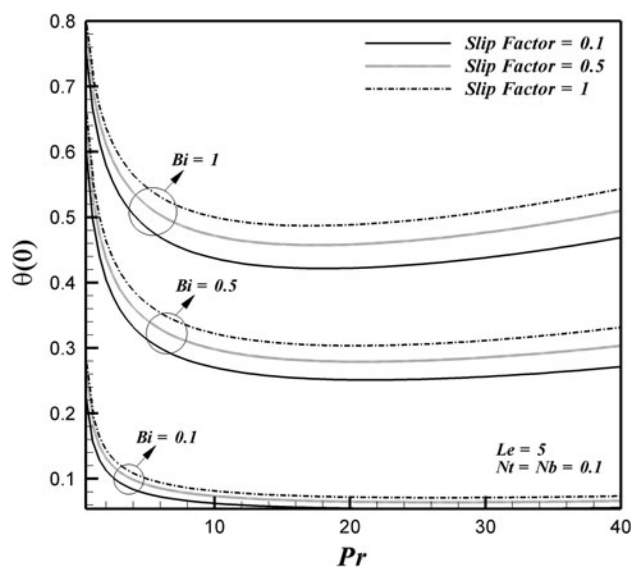

Fig. 8 Effects of slip factor, biot number and Prandtl number on the dimensionless wall temperature for $Le = 5$ and $Nb = 0.1$ and $Nt = 0.1$

dimensionless heat transfer rate, reduced Nusselt number, increases with decrease of the thermophoresis parameter, increase of the Biot number and decrease of the slip factor. Figure 7 depicts that increase of thermophoresis parameter decreases the reduced Sherwood number for small values of Biot number (*i.e.* $Bi \approx 0.1$), but for comparatively large values of the Biot number (*i.e.* $Bi \approx 0.5$) increase of thermophoresis parameter first decreases the reduced Sherwood number and then increases it. In addition, from the Fig. 7 it is clear that increase of the slip factor decreases the reduced Sherwood number. The wall temperature values $\theta(0)$ as a function of Prandtl number for selected values of Biot number and slip factor parameter are plotted in Fig. 8 when $Nb = Nt = 0.1$ and $Le = 5$. This figure depicts that the dimensionless wall temperature increases with increase of Biot number or slip parameter, but it first decreases and then slowly increases with the increase of Prandtl number. Therefore, for each comparatively large value of Biot number there is an optimum Prandtl number which minimizes the dimensionless wall temperature $\theta(0)$.

4 Conclusion

The effect of partial slip (*i.e.* Navier's condition) on the boundary layer flow and heat transfer of nanofluids past stretching sheet prescribed convective heat transfer is theoretically investigated. The boundary layer equations governing the flow, heat and nanoparticle are reduced to a set of nonlinear ordinary differential equations using the similarity transformations. The obtained differential equations are solved numerically for different combinations of nanofluid parameters. Effect of slip factor (λ), Biot number (Bi) and nanofluid parameters including Lewis number (Le), Brownian motion parameter (Nb) and thermophoresis parameter (Nt) on the nanoparticle and thermal boundary layers are discussed using tables and figures. It is observed that by the increase in the slip factor λ and Biot number Bi the thermal boundary layer thickness increased. The reduced Nusselt number and reduced Sherwood number on the stretching sheet are strongly influenced by the slip factor and Biot number. In all cases, the reduced Nusselt number and reduced Sherwood number are decreased with the increase of slip factor λ. The reduced Nusselt number increased with the increase of Biot number and decreased with the increase of thermophoresis parameter for comparatively large values of Prandtl and Lewis numbers. The dimensionless wall temperature increased with increase of the Biot number or slip factor. Finally, it is found that for small values of the Biot number, increase of the thermophoresis parameter decreases the reduced Sherwood number (for comparatively small values of thermophoresis), but when the thermophoresis parameter is comparatively large, the increase of thermophoresis parameter increases the reduced Sherwood number. Therefore, for each value of slip factor and comparatively large values of Biot number (i.e. $Bi \approx 0.5$) and small values of Nb (i.e. $Nb = 0.1$) there is an Nt which minimizes the Sherwood number. In addition, when Nb and Nt are comparatively small, for each comparatively large value of Biot number there is an optimum Prandtl number which minimizes the dimensionless wall temperature $\theta(0)$.

Acknowledgments The authors are grateful to Shahid Chamran University of Ahvaz for its crucial support.

References

1. Fisher EG (1976) Extrusion of plastics. Wiley, New York
2. Altan T, Oh S, Gegel H (1979) Metal forming fundamentals and applications. American Society of Metals
3. Tadmor Z, Klein I (1970) Engineering principles of plasticating extrusion. Van Nostrand Reinhold, New York
4. Karwe MV, Jaluria Y (1991) Numerical simulation of thermal transport associated with a continuous moving flat sheet in materials processing. ASME J Heat Transfer 119:612–619
5. Yacob NA, Ishak A, Pop I, Vajravelu K (2011) Boundary layer flow past a stretching/shrinking surface beneath an external uniform shear flow with a convective surface boundary condition in a nanofluid. Nanoscale Res Lett 6:314–321
6. Eastman JA, Choi SUS, Li S, Yu W, Thompson LJ (2001) Anomalously increased effective thermal conductivities of ethylene glycolbased nanofluids containing copper nanoparticles. Appl Phys Lett 78:718–720
7. Daungthongsuk W, Wongwises S (2007) A critical review of convective heat transfer nanofluids. Renew Sustain Energy Rev 11:797–817
8. Trisaksri V, Wongwises S (2007) Critical review of heat transfer characteristics of nanofluids. Renew Sustain Energy Rev 11:512–523
9. Das SK, Choi S, Yu W, Pradeep T (2007) Nanofluids: science and technology. Wiley, New Jersey
10. Wongcharee K, Eiamsa-ard S (2011) Enhancement of heat transfer using CuO/water nanofluid and twisted tape with alternate axis. Int Commun Heat Mass Transfer 38:742–748
11. Hwang K, Jang S, Choi S (2009) Flow and convective heat transfer characteristics of water-based Al_2O_3 nanofluids in fully developed laminar flow regime. Int J Heat Mass Transfer 52:193–199
12. Pakravan HA, Yaghoubi M (2011) Combined thermophoresis, Brownian motion and Dufour effects on natural convection of nanofluids. Int J Therm Sci 50:394–402
13. Vajravelu K, Prasad KV, Lee J, Lee C, Pop I, Van Gorder RA (2011) Convective heat transfer in the flow of viscous Ag–water and Cu–water nanofluids over a stretching surface. Int J Therm Sci 50:843–851
14. Buongiorno J (2006) Convective transport in nanofluids. J Heat Transfer 128:240
15. Pak BC, Cho Y (1998) Hydrodynamic and heat transfer study of dispersed fluids with submicron metallic oxide particles. Exp Heat Transfer 11:151–170
16. Kakac S, Pramaumjaroenkij A (2009) Review of convective heat transfer enhancement with nanofluids. Int J Heat Mass Transfer 52:3187–3196
17. Xuan Y, Li Q (2003) Investigation on convective heat transfer and flow features of nanofluids. J Heat Transfer 125:151–155
18. Sakiadis BC (1961) Boundary-layer behavior on continuous solid surface: I. Boundary-layer equations for two-dimensional and axisymmetric flow. J AIChe 7:26–33
19. Crane L (1970) Flow past a stretching plate. Z Angew Math Phys 21:645–651
20. Prasad KV, Vajravelu K (2009) Heat transfer in the MHD flow of a power law fluid over a non-isothermal stretching sheet. Int J Heat Mass Transfer 52:4956–4965
21. Sahoo B, Poncet S (2011) Flow and heat transfer of a third grade fluid past an exponentially stretching sheet with partial slip boundary condition. Int J Heat Mass Transfer 54:5010–5019
22. Khan WA, Pop I (2010) Boundary-layer flow of a nanofluid past a stretching sheet. Int J Heat Mass Transfer 53:2477–2483
23. Noghrehabadi A, Pourrajab R, Ghalambaz M (2012) Effect of partial slip boundary condition on the flow and heat transfer of nanofluids past stretching sheet prescribed constant wall temperature. Int J Therm Sci 54:253–261
24. Noghrehabadi A, Ghalambaz M, Ghalambaz M, Ghanbarzadeh A (2012) Comparing thermal enhancement of Ag–water and SiO_2–water nanofluids over an isothermal stretching sheet with suction or injection. J Comput Appl Res Mech Eng 2:35–47
25. Yazdi MH, Abdullah S, Hashim I, Sopian K (2011) Slip MHD liquid flow and heat transfer over non-linear permeable stretching surface with chemical reaction. Int J Heat Mass Transfer 54:3214–3225
26. Gupta PS, Gupta AS (1977) Heat and mass transfer on a stretching sheet with suction or blowing. Can J Chem Eng 55:744–749

27. Fang T, Zhang J (2009) Thermal boundary layers over a shrinking sheet: an analytical solution. Acta Mech 209:325–343
28. Cortell R (2007) Viscous flow and heat transfer over a nonlinearly stretching sheet. Appl Math Comput 184:864–873
29. Aziz A (2009) A similarity solution for laminar thermal boundary layer over a flat plate with a convective surface boundary condition. Commun Nonlinear Sci Numer Simul 14:1064–1068
30. Magyari E (2011) Comment on "A similarity solution for laminar thermal boundary layer over a flat plate with a convective surface boundary condition" by A. Aziz, Comm Nonlinear Sci Numer Simul. 2009;14:1064–1068. Comm Nonlinear Sci Numer Simul 16:599–601
31. Hamad MAA, Ferdows M (2012) Similarity solution of boundary layer stagnation-point flow towards a heated porous stretching sheet saturated with a nanofluid with heat absorption/generation and suction/blowing: a lie group analysis. Commun Nonlinear Sci Numer Simul 17:132–140
32. Ishak A (2010) Similarity solutions for flow and heat transfer over a permeable surface with convective boundary condition. Appl Math Comput 217:837–842
33. Merkin JH, Pop I (2011) The forced convection flow of a uniform stream over a flat surface with a convective surface boundary condition. Commun Nonlinear Sci Numer Simul 16:3602–3609
34. Yao S, Fang T, Zhong Y (2011) Heat transfer of a generalized stretching/shrinking wall problem with convective boundary conditions. Commun Nonlinear Sci Numer Simul 16:752–760
35. Mukhopadhyay S, Gorla RSR (2012) Effects of partial slip on boundary layer flow past a permeable exponential stretching sheet in presence of thermal radiation. Heat Mass Transfer 48:1773–1781
36. Wang CY (2002) Flow due to a stretching boundary with partial slip—an exact solution of the Navier–Stokes equations. Chem Eng Sci 57:3745–3747
37. Wang CY (2009) Analysis of viscous flow due to a stretching sheet with surface slip and suction. Nonlinear Anal Real World Appl 10:375–380
38. Andersson HI (2002) Slip flow past a stretching surface. Acta Mech 158:121–125
39. Ariel PD (2007) Axisymmetric flow due to a stretching sheet with partial slip. Comput Math Appl 54:1169–1183
40. Sahoo B, Do Y (2010) Effects of slip on sheet-driven flow and heat transfer of a third grade fluid past a stretching sheet. Int Commun Heat Mass Transfer 37:1064–1071
41. Hayat T, Qasim M, Mesloub S (2011) MHD flow and heat transfer over permeable stretching sheet with slip conditions. Int J Numer Methods Fluids 66:963–975
42. Das K (2012) Impact of thermal radiation on MHD slip flow over a flat plate with variable fluid properties. Heat Mass Transfer 48:767–778
43. Bocquet L, Barrat JL (2007) Flow boundary conditions from nano- to micro-scales. Soft Matter 3:685–693
44. Bachok N, Ishak A, Pop I (2010) Boundary-layer flow of nanofluids over a moving surface in a flowing fluid. Int J Therm Sci 49:1663–1668
45. Kuznetsov AV, Nield DA (2010) Natural convective boundary-layer flow of a nanofluid past a vertical plate. Int J Therm Sci 49:243–247
46. Hassani M, Mohammad Tabar M, Nemati H, Domairry G, Noori F (2011) An analytical solution for boundary layer flow of a nanofluid past a stretching sheet. Int J Therm Sci 50:2256–2263
47. Makinde OD, Aziz A (2011) Boundary layer flow of a nanofluid past a stretching sheet with a convective boundary condition. Int J Therm Sci 50:1326–1332
48. Noghrehabadi A, Saffarian MR, Pourrajab R, Ghalambaz M (2013) Entropy analysis for nanofluid flow over a stretching sheet in the presence of heat generation/absorption and partial slip. J Mech Sci Technol 27:927–937
49. Noghrehabadi A, Ghalambaz M, Ghanbarzadeh A (2012) Heat transfer of magnetohydrodynamic viscous nanofluids over an isothermal stretching sheet. J Thermophys Heat Transfer 26:686–689
50. Rana P, Bhargava R (2012) Flow and heat transfer of a nanofluid over a non-linearly stretching sheet: a numerical study. Commun Nonlinear Sci Numer Simul 17:212–226
51. Majumder M, Chopra N, Andrews R, Hinds BJ (2005) Nanoscale hydrodynamics: enhanced flow in carbon nanotubes. Nature 438:44
52. Van Gorder RA, Sweet E, Vajravelu K (2010) Nano boundary layers over stretching surfaces. Commun Nonlinear Sci Numer Simulat 15:1494–1500
53. Fehlberg E (1969) Low-order classical Runge–Kutta formulas with step size control and their application to some heat transfer problems. Technical report NASA
54. Fehlberg E (1970) Klassische Runge-Kutta-Formeln vierter und niedrigerer Ordnung mit Schrittweiten-Kontrolle und ihre Anwendung auf Wärmeleitungsprobleme. Comput Arch Elektron Rechn 6:61–71
55. Hamad MAA, Uddin MJ, Ismail AIM (2012) Investigation of combined heat and mass transfer by Lie group analysis with variable diffusivity taking into account hydrodynamic slip and thermal convective boundary conditions. Int J Heat Mass Transfer 55:1355–1362
56. Nield DA, Kuznetsov AV (2009) The Cheng–Minkowycz problem for natural convective boundary-layer flow in a porous medium saturated by a nanofluid. Int J Heat Mass Transfer 52:2795–5792